

WIRELESSLY POWERING: THE FUTURE

Gain expressions for resonant inductive wireless power transfer links with one relay element

FRANCO MASTRI¹, MAURO MONGIARDO², GIUSEPPINA MONTI³, MARCO DIONIGI²
AND LUCIANO TARRICONE³

In this paper, a resonant inductive wireless power transfer link using a relay element is analyzed. Different problems of practical interest are considered and solved by modeling the link as a lossy two-port network. According to the two-port network formalism, the standard gain definition (i.e. the power, the available, and the transducer gains) are used for describing the network behavior. Firstly, the case of a link with given parameters is considered and the analytical expressions of the optimal terminating impedances for maximizing the link gains are derived. Later on, the case of a link with given source and load is analyzed and the possibility of maximizing the performance by acting either on the transmitting or on the receiving side is investigated. It is shown that by using a single relay element, it is not always possible to maximize all the figures of merit that could be of interest in the WPT context. Theoretical data are validated by comparisons with circuital simulation results.

Keywords: Wireless power transfer, Resonant inductive coupling, Relay element, Gains

Received 30 April 2017; Revised 1 September 2017; Accepted 1 September 2017; first published online 12 October 2017

I. INTRODUCTION

Wireless power transfer (WPT) is increasingly recognized from both academia and industry as a promising solution for the recharging of electronic systems without a physical connection to a power grid [1–7].

Among the possible strategies, for applications where the goal is a contactless recharge, the attention has been focused on the use of resonant inductively coupled systems, which allow maximizing the performance for mid-range WPT links [8–12].

In this regard, the case of two inductively coupled resonators has been deeply investigated in the literature. In particular, in [10] the expression of the load impedance which allows maximizing either the power on the load or the efficiency has been derived for a link with assigned parameters. In [13], the equations for designing the optimum link for given values of the source have been reported.

However, although the results reported in the literature demonstrate that for the case of a two-coil link both the power on the load or the efficiency can be maximized by appropriately setting the relevant parameters, the efficiency quickly drops as the transfer distance increases.

Accordingly, the use of multi-resonator systems, where one or more relay resonators are added between the transmitting and the receiving ones, has been proposed as a viable strategy for increasing the transfer distance [14–27]. In particular, in [21] the case of a multi-resonator WPT link in a domino arrangement is studied; the analytical expressions of the optimal load and maximum efficiency are derived. It is also experimentally demonstrated the possibility of controlling the power flow in a multi-coil link in various domino arrangements (i.e. straight, curved, circular, and y -shaped). In [28], the case of a multi-resonator link with a single transmitter and multiple receivers is investigated demonstrating that the number of resonators influences the power division ratio of each receiver.

However, the most analyzed case is the one of a link using either three or four resonators. In this regard, in [22] the case of a four-resonator scheme achieved by using two relay resonators has been experimentally investigated demonstrating the possibility of improving the efficiency with respect to the basic scheme using just two resonators.

In [23], an asymmetrical four-coil link is theoretically investigated. It is shown that for a desired value of the efficiency, there is a maximum operating distance which can be achieved; similarly, for a given operating distance there is a maximum value of the efficiency which can be realized.

In [24, 26] the case of a three-resonator link has been analyzed. More specifically, in [24] the coupled mode theory has been used for deriving the efficiency corresponding to different configurations of the relay element with respect to the transmitting and the receiving resonators; the reported results

¹Department of Electrical, Electronic and Information Engineering “Guglielmo Marconi”, University of Bologna, Bologna, Italy. Phone: +39 0832 29 7365

²Department of Engineering, University of Perugia, Italy

³Department of Engineering for Innovation, University of Salento, Italy

Corresponding author:

G. Monti

Email: giuseppina.monti@unisalento.it

demonstrate that the use of the intermediate resonator allows improving the efficiency even in the case where it is perpendicularly arranged with respect to the two-resonator link.

Similarly, in [25] the advantages of a three-coil link are exploited in the context of medical implants. The idea suggested in [26] is to use the relay resonator to shift the current stress from the transmitting resonator to the relay element in such a way to improve the magnetic coupling with the receiving coil.

In [27], based on the reflected load theory, a design procedure for maximizing the efficiency of a link using three and four resonators has been proposed. The performance of the network is described in terms of the two common figures of merit usually adopted for the analysis of WPT links, namely the power transfer efficiency and the active power delivered to the load.

According to the theoretical results achieved for the power on the load and the efficiency of these two schemes, the authors conclude that the three-coil configuration provides the best compromise for the achievable performance in terms of power on the load and efficiency.

This discussion is further deepened in the present paper, where an alternative approach is proposed for solving the same problem. In more detail, the case of a three-resonator link is considered; as in [27], the three-resonator link is described as a lossy linear two-port network and the relay element is treated as a further degree of freedom of the system, which can be used to optimize the performance. With respect to the analysis proposed in [27], in the present paper, the gain definitions usually adopted in the context of two-port active networks are used for describing the network behavior. It is shown that this approach is completely equivalent to the description of the network based on the power transfer efficiency and active power on the load. However, the use of three gain definitions that are well established and consolidated in the literature has two main advantages: (1) it eliminates possible ambiguity related to the definition of the variables of interest in the efficiency calculation; (2) it simplifies the calculation and the optimization of the figures of merit of interest. In fact, the three gain definitions adopted in the present paper are usually available in common circuital simulators.

The relevant design equations for the best configuration of the relay element are derived; the best design is expressed in terms of closed form equations of the coupling coefficients of the relay element with the transmitting and the receiving resonators. It is shown that the three-resonator scheme does not allow the analytical maximization of all the figures of merit that could be of interest in the WPT context.

The paper is organized as follows: in Section II, the relevant gain definitions are introduced; in Section III, the definition of conjugate image impedances of a two-port network is briefly recalled and the conditions for maximizing the gains of the network are given and discussed. In Section IV, the analyzed problem is introduced and analytical formulas are derived for the solutions of interest. Later on, in Section V, the theory is validated through circuital simulations; finally, conclusions are drawn in Section VI.

II. GAIN DEFINITIONS FOR TWO-PORT NETWORKS

A two-port network, realized either without relay elements or with one or more relay elements, is advantageously described

by gain functions. The latter description is commonly used for amplifiers and can naturally be employed also in the context of WPT. In this section, after a brief definition of the relevant quantities, the most commonly used gain definitions are introduced.

It is assumed that the two-port network realizing WPT is known and a description is available in terms, e.g., of its impedance parameters

$$z_{ij} = r_{ij} + jx_{ij} \quad (1)$$

with $(i, j) = 1, 2$. It is also assumed that the input and output ports are connected to a sinusoidal voltage generator V_G with internal impedance $Z_G = R_G + jX_G$, and to a load impedance $Z_L = R_L + jX_L$, respectively.

In order to derive the gain functions, it is convenient to represent the two-port network by the Thévenin equivalent circuit depicted in Fig. 1. To this end, the current I_2 on the secondary side is first derived as:

$$I_2 = -\frac{z_{21}}{z_{22} + Z_L} I_1, \quad (2)$$

which allows to obtain the following expression for the input impedance:

$$Z_{in} = R_{in} + jX_{in} = \frac{V_1}{I_1} = z_{11} - \frac{z_{12}z_{21}}{z_{22} + Z_L}. \quad (3)$$

The voltage on the secondary side may be then written as:

$$V_2 = \left(z_{22} - \frac{z_{12}z_{21}}{z_{11} + Z_G} \right) I_2 + \frac{z_{21}}{z_{11} + Z_G} V_G, \quad (4)$$

which provides the following expression when the generator is short circuited:

$$Z_{out} = \frac{V_2}{I_2} \Big|_{V_G=0} = z_{22} - \frac{z_{12}z_{21}}{z_{11} + Z_G}. \quad (5)$$

Finally, the Thévenin equivalent voltage is readily obtained as:

$$V_{th} = V_2 \Big|_{I_2=0} = \frac{z_{21}}{z_{11} + Z_G} V_G. \quad (6)$$

Referring to Fig. 1, which illustrates the powers of interest, in the following part of this section, the relevant gain definitions will be introduced.

A) Power gain

The power gain is defined as the ratio between the power delivered to the load and the input power to the two-port network:

$$G_P = \frac{P_L}{P_{in}}. \quad (7)$$

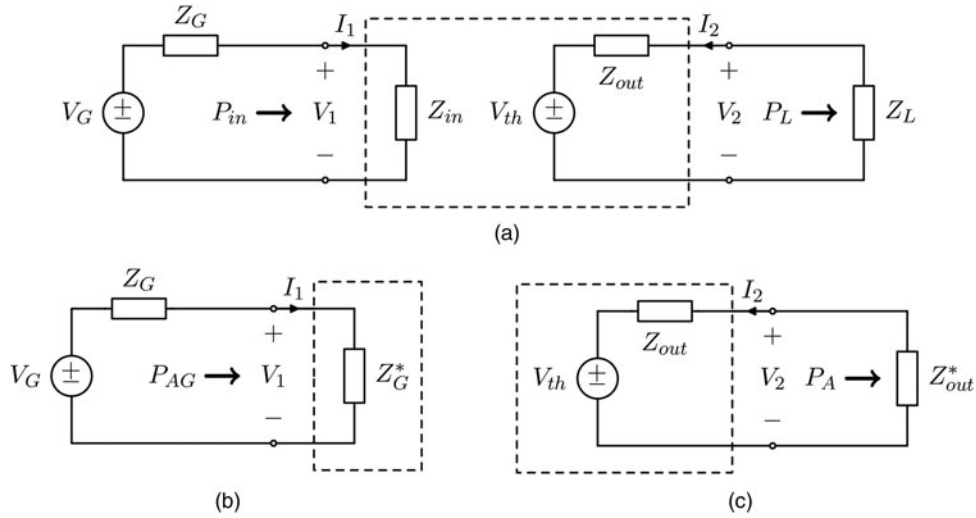


Fig. 1. (a) Equivalent circuit of a two-port network with Thévenin representation. (b) Definition of the available generator power P_{AG} . (c) Definition of the available output power P_A .

The input power is readily evaluated as:

$$P_{in} = \frac{1}{2} R_{in} |I_1|^2, \quad (8)$$

and the output power is given by:

$$P_L = \frac{1}{2} R_L |I_2|^2. \quad (9)$$

The power gain can therefore be expressed as:

$$G_p = \frac{R_L}{R_{in}} \left| \frac{I_2}{I_1} \right|^2 = \frac{R_L}{R_{in}} \left| \frac{z_{21}}{z_{22} + Z_L} \right|^2. \quad (10)$$

It is noted that G_p depends on the load impedance Z_L , but does not depend on the generator impedance Z_G . In addition, in the WPT context, the power gain is often identified with the efficiency η [27].

B) Available gain

Another gain expression is the available power gain, which is defined as the ratio between the maximum available load power P_A and the available input power P_{AG} :

$$G_A = \frac{P_A}{P_{AG}}. \quad (11)$$

The available input power P_{AG} is given by:

$$P_{AG} = \frac{|V_G|^2}{8R_G}, \quad (12)$$

while the maximum available load power P_A is:

$$P_A = \frac{|V_{th}|^2}{8R_{out}}. \quad (13)$$

Hence, their ratio provides:

$$G_A = \frac{R_G}{R_{out}} \left| \frac{V_{th}}{V_G} \right|^2 = \frac{R_G}{R_{out}} \left| \frac{z_{21}}{z_{11} + Z_G} \right|^2. \quad (14)$$

It can be noted that the available gain is only related to the generator impedance, and does not depend on the load impedance.

C) Transducer gain

The transducer gain of a two-port network is defined by the relation:

$$G_T = \frac{P_L}{P_{AG}}. \quad (15)$$

By deriving I_2 as a function of V_G :

$$I_2 = \frac{V_{th}}{Z_{out} + Z_L} = \frac{z_{21} V_G}{(z_{11} + Z_G)(z_{22} + Z_L) - z_{12} z_{21}} \quad (16)$$

and replacing this expression in (9), one obtains:

$$G_T = \frac{4|z_{21}|^2 R_G R_L}{|(z_{11} + Z_G)(z_{22} + Z_L) - z_{12} z_{21}|^2}. \quad (17)$$

This expression shows that G_T depends both on Z_G and Z_L .

From the definition of G_T given in (15), it can be observed that, if the available power is fixed, maximizing the transducer gain is equivalent to maximize the power on the load P_L . In fact, G_T is quantitatively coincident with the power delivered to the load for $P_{AG} = 1$ W. It should also be noted that, in order to keep P_{AG} constant, if R_G is varied, V_G has to be varied accordingly, as it happens when a matching network is inserted between the generator and the input port.

This shows that the two approaches usually adopted in the WPT context (i.e. the one aiming at maximizing the efficiency of the link and the one aiming at maximizing the power on the load) are equivalent to maximize either G_p or G_T .

III. CONJUGATE IMAGE IMPEDANCES OF A TWO-PORT NETWORK AND GAINS MAXIMIZATION

In this section, the conditions for maximizing the gains defined in Table 1 will be discussed. To this end, it is useful to recall the definition of conjugate image impedances of a two-port network [29, 30].

A) Conjugate image impedances

The conjugate image impedances of a two-port network, Z_{c1} and Z_{c2} , are defined as in Fig. 2. When port 2 is terminated on Z_{c2} , the input impedance seen from port 1 is the complex conjugate of Z_{c1} (i.e. Z_{c1}^*); similarly, when port 1 is terminated on Z_{c1} , the input impedance seen from port 2 is the complex conjugate of Z_{c2} (i.e. Z_{c2}^*). The conjugate image impedances are an intrinsic property of the two-port network and, by using the terms of the impedance matrix, can be expressed as [30]:

$$Z_{c1} = R_{c1} + jX_{c1} = r_{11}(\theta_r + j\theta_x) - jx_{11}, \quad (18)$$

$$Z_{c2} = R_{c2} + jX_{c2} = r_{22}(\theta_r + j\theta_x) - jx_{22}, \quad (19)$$

where the following definitions have been used:

$$\theta_r = \sqrt{\left(1 - \frac{r_c^2}{r_{11}r_{22}}\right)\left(1 + \frac{x_c^2}{r_{11}r_{22}}\right)}, \quad (20)$$

$$\theta_x = \frac{r_c x_c}{r_{11}r_{22}}, \quad (21)$$

$$r_c = \text{Re}\{\sqrt{z_{12}z_{21}}\}, \quad (22)$$

$$x_c = \text{Im}\{\sqrt{z_{12}z_{21}}\}. \quad (23)$$

It is worth observing that in the case where the terms of the impedance matrix are real quantities (i.e. the terms $x_{ij} = 0$, $(i, j) = 1, 2$), the complex conjugate image impedances become purely resistive quantities, and are referred to as image resistances. Another particular case, which is frequently encountered in the WPT context, where Z_{c1} and Z_{c2} are purely resistive, is that where z_{11} and z_{22} are real, while z_{12} and z_{21} are purely imaginary.

B) Maximization of the gains for a generic two-port network

According to the definitions given in Table 1, it can be shown that:

- the power gain G_P is independent of Z_G , while it depends on Z_L and is maximized for $Z_L = Z_{c2}$;
- the available gain G_A is independent of Z_L , while it depends on Z_G and is maximized for $Z_G = Z_{c1}$.

As per the transducer gain G_T , since

$$\begin{aligned} P_L &\leq P_A, \\ P_{in} &\leq P_{AG}, \end{aligned} \quad (24)$$

it results

$$\begin{aligned} G_T &\leq G_P, \\ G_T &\leq G_A. \end{aligned} \quad (25)$$

In particular, it can be noted that:

- $G_T = G_P$ if the power-matching condition $Z_G = Z_{in}^*$ is realized at the input port;
- $G_T = G_A$ if the power-matching condition $Z_L = Z_{out}^*$ is realized at the output port;

Table 1. Gain definitions and expressions.

	Definition	General expression	Three-coil WPT link
G_P	$\frac{P_L}{P_{in}}$	$\frac{R_L}{R_{in}} \left \frac{z_{21}}{z_{22} + Z_L} \right ^2$	$\frac{\chi_{13}^2 \chi_{32T}^2}{(\chi_{13}^2 + \chi_{32T}^2 + 1)(\chi_{32T}^2 + 1)} \frac{Q_{2T}}{Q_L}$
G_A	$\frac{P_A}{P_{AG}}$	$\frac{R_G}{R_{out}} \left \frac{z_{21}}{z_{11} + Z_G} \right ^2$	$\frac{Q_{1T}}{Q_G} \frac{\chi_{1T3}^2 \chi_{32}^2}{(\chi_{1T3}^2 + 1)(\chi_{1T3}^2 + \chi_{32}^2 + 1)}$
G_T	$\frac{P_L}{P_{AG}}$	$\frac{4 z_{21} ^2 R_G R_L}{ (z_{11} + Z_G)(z_{22} + Z_L) - z_{12}z_{21} ^2}$	$\frac{Q_{1T}}{Q_G} \frac{4\chi_{1T3}^2 \chi_{32T}^2}{(\chi_{1T3}^2 + \chi_{32T}^2 + 1)^2} \frac{Q_{2T}}{Q_L}$

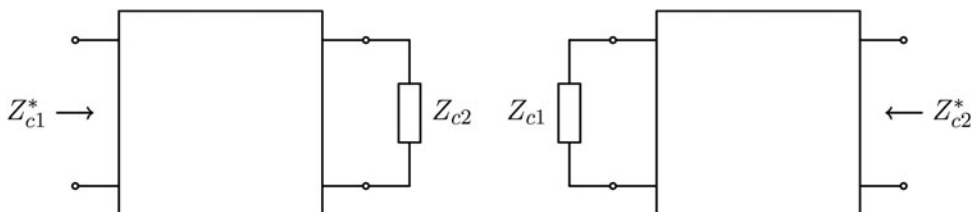


Fig. 2. Conjugate image impedances as defined in [30].

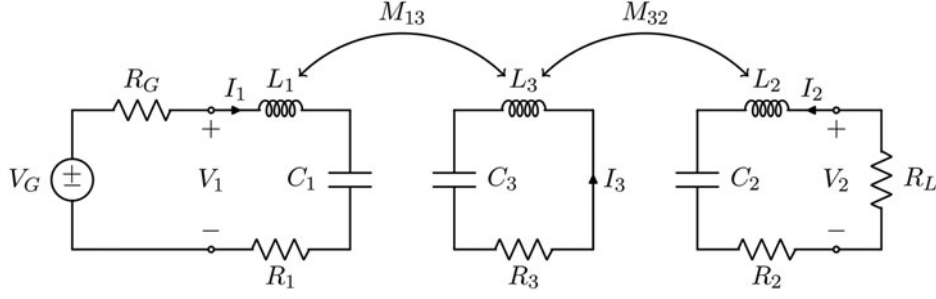


Fig. 3. Schematic of the WPT link with one relay element.

- $G_T = G_P = G_A$ if the power-matching condition is realized at both the input and the output ports, which requires $Z_G = Z_{c1}$ and $Z_L = Z_{c2}$.

Hence, it can be concluded that:

- if Z_G (or Z_L) is fixed, the maximum value of G_T is obtained for $Z_L = Z_{out}^*$ (or $Z_G = Z_{in}^*$);
- if both Z_G and Z_L can be optimized, the maximum values of G_T is obtained for $Z_G = Z_{c1}$ and $Z_L = Z_{c2}$.

The previous discussion also shows that the maximum of G_P with respect to (w.r.t.) Z_L , the maximum of G_A w.r.t. Z_G , and the maximum of G_T w.r.t. Z_G and Z_L are equal. In the following their common value will be denoted by G_M .

IV. WPT WITH ONE RELAY ELEMENT

A) Problem description

The problem analyzed in this paper is schematically represented in Fig. 3. The case of a resonant inductive WPT link with a relay element is considered. It is assumed that the link is driven by a sinusoidal voltage generator with angular frequency ω_0 and internal resistance R_G , and that it is connected to a purely resistive load R_L .

In the following, the transmitting (TX) resonator is denoted by 1, the receiving resonator (RX) by 2, the relay resonator, placed between the TX and the RX resonators, is denoted by 3. It is assumed that the three coils are synchronous and resonate at the angular frequency ω_0 .

The symbols defined in Table 2 are used for the analysis. For each resonator, the loss resistance is denoted by R_i and the unloaded quality factor by Q_i . The external quality factors of the TX and RX resonators are indicated by Q_G and Q_L , respectively, while the corresponding loaded quality factors are indicated by Q_{1T} and Q_{2T} . The coupling coefficient

between coils i and j is denoted by k_{ij} ; it is assumed that only adjacent coils are coupled, i.e. only k_{13} and k_{32} are different from zero, while $k_{12} = 0$. The reactance of the inductor at the receiving side, $X_0 = \omega_0 L_2$, is used for normalization. The parameters n_{ij} represent the transformation ratios. Finally, the symbols χ_{ij} , χ_{1T3} , and χ_{32T} are also introduced, in order to alleviate the notation.

In this paper, the following problems will be considered and solved.

- CASE A – Assuming that the parameters of the link (and therefore the couplings k_{13} and k_{32}) are given, find the optimal values of R_G and R_L for maximizing the gains of the network.
- CASE B – Assuming that the load and the generator impedances are given, try to maximize the gains of the two-port network by acting either on the receiving side (i.e. by optimizing k_{32}) or on the transmitting side (i.e. by optimizing k_{13}).

All the above cases may include, or may not, a communication between the TX and the RX in the optimization phase.

1) IMPEDANCE MATRIX OF A THREE-COIL LINK

At the operating angular frequency ω_0 , the equations for the three-coil link are

$$\begin{aligned} V_1 &= R_1 I_1 + j\omega_0 M_{13} I_3, \\ V_2 &= R_2 I_2 + j\omega_0 M_{32} I_3, \\ 0 &= j\omega_0 M_{13} I_1 + j\omega_0 M_{32} I_2 + R_3 I_3. \end{aligned} \quad (26)$$

From (26), making use of the definition reported in Table 2, the following expressions can be derived for the parameters of the link impedance matrix:

$$\begin{aligned} z_{11} &= r_{11} = \frac{X_0 n_{12}^2}{Q_1} (\chi_{13}^2 + 1), \\ z_{12} &= z_{21} = r_{12} = \frac{X_0 n_{12}}{\sqrt{Q_1 Q_2}} \chi_{13} \chi_{32}, \\ z_{22} &= r_{22} = \frac{X_0}{Q_2} (\chi_{32}^2 + 1). \end{aligned} \quad (27)$$

It can be noted that all the elements of the impedance matrix are real.

2) INPUT AND OUTPUT RESISTANCES

Since the terminating impedances are assumed to be purely resistive, also the input and output impedances of the three-

Table 2. Definitions.

$X_0 = \omega_0 L_2$	$n_{ij} = \sqrt{\frac{L_i}{L_j}}$	$k_{ij} = \frac{M_{ij}}{\sqrt{L_i L_j}}$
$Q_i = \frac{\omega_0 L_i}{R_i}$	$Q_G = \frac{\omega_0 L_1}{R_G}$	$Q_L = \frac{\omega_0 L_2}{R_L}$
$Q_{1T} = \frac{Q_1 Q_G}{Q_1 + Q_G}$	$Q_{2T} = \frac{Q_2 Q_L}{Q_2 + Q_L}$	
$\chi_{ij} = \sqrt{Q_i Q_j} k_{ij}$	$\chi_{1T3} = \sqrt{Q_{1T} Q_3} k_{13}$	$\chi_{32T} = \sqrt{Q_3 Q_{2T}} k_{32}$

coil link are real. From (27), by means of (3) and (5), their expressions can be derived as

$$R_{in} = \frac{X_0 n_{12}^2 \chi_{13}^2 + \chi_{32T}^2 + 1}{Q_1 \chi_{32T}^2 + 1}, \quad (28)$$

$$R_{out} = \frac{X_0 \chi_{1T3}^2 + \chi_{32}^2 + 1}{Q_2 \chi_{1T3}^2 + 1}. \quad (29)$$

3) CONJUGATE IMAGE IMPEDANCES

As previously stated, since all the terms of the impedance matrix of a three-coil WPT link are purely real, the conjugate image impedances are simply the image resistances, and can be derived by (18) and (19) as:

$$Z_{c1} = R_{i1} = \frac{X_0 n_{12}^2}{Q_1} \sqrt{\frac{(\chi_{13}^2 + 1)(\chi_{13}^2 + \chi_{32}^2 + 1)}{\chi_{32}^2 + 1}}, \quad (30)$$

$$Z_{c2} = R_{i2} = \frac{X_0}{Q_2} \sqrt{\frac{(\chi_{32}^2 + 1)(\chi_{13}^2 + \chi_{32}^2 + 1)}{\chi_{13}^2 + 1}}. \quad (31)$$

4) POWER GAIN, AVAILABLE GAIN, AND TRANSDUCER GAIN

The expressions of the gains for a three-coil WPT link can be calculated by substituting (27) in the general expressions summarized in Table 1. For the power gain, the following expression can be obtained:

$$G_p = \frac{\chi_{13}^2 \chi_{32T}^2}{(\chi_{13}^2 + \chi_{32T}^2 + 1)(\chi_{32T}^2 + 1)} \frac{Q_{2T}}{Q_L}. \quad (32)$$

The expression of the available gain is:

$$G_A = \frac{Q_{1T}}{Q_G} \frac{\chi_{1T3}^2 \chi_{32}^2}{(\chi_{1T3}^2 + 1)(\chi_{1T3}^2 + \chi_{32}^2 + 1)}. \quad (33)$$

Finally, the expression of the transducer gain is:

$$G_T = \frac{Q_{1T}}{Q_G} \frac{4\chi_{1T3}^2 \chi_{32T}^2}{(\chi_{1T3}^2 + \chi_{32T}^2 + 1)^2} \frac{Q_{2T}}{Q_L}. \quad (34)$$

B) CASE A: optimal load impedance for a three-coil link

According to the results obtained for a generic two-port network, the power gain G_p is maximized for $R_L = R_{i2}$ given by (31), the available gain G_A is maximized for $R_G = R_{i1}$ given by (30), and the transducer gain G_T is maximized for $R_G = R_{i1}$ and $R_L = R_{i2}$. When the previous conditions are satisfied, the three gains assume the same maximum value, which can be expressed as

$$G_M = \frac{\left[\sqrt{\chi_{13}^2 + \chi_{32}^2 + 1} - \sqrt{(\chi_{13}^2 + 1)(\chi_{32}^2 + 1)} \right]^2}{\chi_{13}^2 \chi_{32}^2}. \quad (35)$$

As per the transducer gain, if the load resistance is fixed, its maximum w.r.t. R_G is obtained when $R_G = R_{i1}$ given by (28), and is equal to G_p given by (32). Analogously, if the generator resistance is fixed, the maximum of G_T w.r.t. R_L is obtained when $R_L = R_{i2}$ given by (29), and is equal to G_A given by (33).

C) CASE B: optimizing a three-coil link when the source and the load are given

In most cases of practical interest, the source and the load are given and can not be freely selected to maximize the performance of the link.

In these cases, the parameters of the link have to be used for maximizing the performance. In this regard, a viable solution is to act on the couplings of the relay element with the primary and the secondary resonators. In particular, one of the two couplings could be used for satisfying the requirement on the transfer distance and the other one to maximize the performance of the link. Accordingly, two different scenarios are of interest:

- it is possible to use k_{13} to satisfy the requirement on the transfer distance and to act on the receiving side by modifying the magnetic coupling k_{32} to maximize the performance;
- it is possible to use k_{32} to satisfy the requirement on the transfer distance and to act on the transmitting side by modifying the magnetic coupling k_{13} to maximize the performance.

1) OPTIMIZING THE COUPLING BETWEEN RELAY AND RECEIVING COIL

Assuming that k_{13} is set according to the requirement on the distance to be covered by the link, the possibility to act on k_{32} to maximize the performance in terms of one of the three gains of the network is investigated.

Power gain

The value of k_{32} which maximizes G_p (i.e. the efficiency of the link) is obtained by equating to zero the derivative of (32) w.r.t. k_{32} :

$$k_{32}^{GP} = \frac{\sqrt{\chi_{13}^2 + 1}}{\sqrt{Q_{2T} Q_3}}. \quad (36)$$

It can be easily verified that the results expressed in (36) is equivalent to that given in equation (25) of [27]. For $k_{32} = k_{32}^{GP}$ the value of G_p becomes

$$G_{P32}^M = \frac{(1 - \sqrt{\chi_{13}^2 + 1})^2}{\chi_{13}^2} \frac{Q_{2T}}{Q_L}. \quad (37)$$

This solution is physically realizable for $k_{32}^{GP} < 1$, i.e.:

$$Q_{2T} > \frac{\sqrt{\chi_{13}^2 + 1}}{Q_3}. \quad (38)$$

According to (38), it is possible to maximize G_P by acting on the receiving side only if Q_L is not too small, this being equivalent to require that R_L is smaller than a value which depends on k_{13} . In more detail, the upper value of R_L decreases with k_{13} ; hence, for a given R_L the maximization of G_P as function of k_{32} may become unfeasible for high values of k_{13} .

Additionally, it can be verified that in (37) the first factor is the maximum value of G_P for the two-coil link formed by resonators 1 and 3 (see the Appendix), while the second factor is the efficiency of resonator 2. This means that optimizing G_P by setting $k_{32} = k_{32}^{GP}$ is equivalent to use resonator 2 for realizing a matching network, which transforms the load R_L into the reflected resistance

$$R_{R,out} = \frac{(\omega_0 M_{32})^2}{R_L + R_2} = \frac{X_0 n_{32}^2}{Q_3} \sqrt{\chi_{13}^2 + 1}, \quad (39)$$

corresponding to the image resistance R_{i2} of the link formed by resonators 1 and 3.

Available gain

The derivative of the available gain w.r.t. k_{32} is zero only for $k_{32} = 0$, which means that it is not feasible to analytically maximize also the available gain for a given k_{13} ; G_A keeps growing as k_{32} increases.

Transducer gain

The value of k_{32} , which maximizes the transducer gain, can be calculated by equating to zero the derivative of (34) w.r.t. k_{32} :

$$k_{32}^{GT} = \sqrt{\frac{\chi_{1T3}^2 + 1}{Q_{2T} Q_3}}. \quad (40)$$

When k_{32} is set according to (40), G_T assumes the value:

$$G_{T32}^M = \frac{Q_{1T}}{Q_G} \frac{\chi_{1T3}^2}{\chi_{1T3}^2 + 1} \frac{Q_{2T}}{Q_L}. \quad (41)$$

It is worth observing that, by measuring the power on the load, it is possible to perform experimentally this optimization without communication with the transmitting side. The value of k_{32} expressed in (40) is physically realizable (i.e. $k_{32}^{GT} < 1$) for:

$$Q_{2T} > \frac{\chi_{1T3}^2 + 1}{Q_3}. \quad (42)$$

Accordingly, by acting on the receiving side, it is possible to maximize G_T for values of Q_{2T} satisfying (42), this corresponding to impose an upper limit to R_L . As evident from (42), the upper limit on R_L depends on k_{13} and lowers for increasing values of k_{13} . Consequently, for a given R_L the solution may become unfeasible for high values of k_{32} .

It can also be observed that the expression (41) of G_{T32}^M can be interpreted as the product of the maximum transducer gain of the two-coil link formed by resonators 1 and 3 w.r.t. its load resistance (see the Appendix), and the efficiency of resonator 2.

This means that the coupled resonators 2 and 3 act as a lossy matching network, which transforms the load resistance R_L into the reflected resistance:

$$R_{R,out} = \frac{(\omega_0 M_{32})^2}{R_L + R_2} = \frac{X_0 n_{32}^2}{Q_3} (\chi_{1T3}^2 + 1), \quad (43)$$

which is equal to the output resistance of the two-coil link formed by resonators 1 and 3. Hence k_{32}^{GT} realizes the power-matching condition at the output port of the link formed by coils 1 and 3. However, it can be noted that in these conditions, the output port impedance of the three-coil link is not matched. In fact, for $k_{32} = k_{32}^{GT}$ it results

$$R_{out} = X_0 \left(\frac{2}{Q_2} + \frac{1}{Q_L} \right) = R_L + 2R_2, \quad (44)$$

hence R_{out} becomes equal to the load resistance only if the RX resonator losses tend to zero. Nevertheless, the non-optimal power transfer at the output port is compensated by the optimal transducer gain of the first two-coil link. As a result, in these conditions, the best three-coil link which can be realized by simply varying k_{32} is obtained.

2) OPTIMIZING THE COUPLING BETWEEN RELAY AND TRANSMITTING COIL

In this case, it is assumed that k_{32} is set to satisfy the requirement on the distance to be covered by the link, and the possibility to use k_{32} to maximize the performance in terms of the three gains of the two-port network is investigated.

Power gain

The derivative of the power gain w.r.t. k_{13} is zero only for $k_{13} = 0$, hence G_P keeps growing as k_{13} increases. As a consequence, it is not feasible to maximize G_P by acting on the transmitting side, while keeping constant k_{32} .

Available gain

For a given value of k_{32} , the available gain G_A can be optimized for

$$k_{13}^{GA} = \frac{\sqrt[4]{\chi_{32}^2 + 1}}{\sqrt{Q_{1T} Q_3}}. \quad (45)$$

The corresponding maximum value of G_A is:

$$G_{A14}^M = \frac{Q_{1T}}{Q_G} \frac{\left(1 - \sqrt{\chi_{32}^2 + 1}\right)^2}{\chi_{32}^2}. \quad (46)$$

The solution expressed in (46) is physically realizable for $k_{13}^{GA} < 1$, which requires:

$$Q_{1T} > \frac{\sqrt{\chi_{32}^2 + 1}}{Q_3}. \quad (47)$$

Hence, similarly to G_T with varying k_{32} , it is possible to maximize G_A by acting on the transmitting side only if R_G is not too large. The upper value of R_G decreases with k_{32} and k_{13}^{GA} may become physically not realizable for high values of k_{32} .

It is worth noticing that in (46), the first factor is the efficiency of the resonator 1, while the second factor is the maximum value of G_A for the two-coil link formed by

resonators 3 and 2 (see the Appendix for the expression of G_A for a two-coil link).

Accordingly, it can be seen that for $k_{13} = k_{13}^{GA}$ the coupled resonators 1 and 2 transform the generator resistance R_G into the reflected resistance

$$R_{R,in} = \frac{(\omega_0 M_{13})^2}{R_G + R_1} = \frac{X_0 n_{32}^2}{Q_3} \sqrt{\chi_{32}^2 + 1}, \quad (48)$$

which is equal to the image resistance R_{i1} of the link formed by resonators 2 and 3.

Transducer gain

The derivative of (34) with respect to k_{13} is zero for

$$k_{13}^{GT} = \sqrt{\frac{\chi_{32T}^2 + 1}{Q_{1T} Q_3}}, \quad (49)$$

giving the following value of the transducer gain

$$G_{T13}^M = \frac{Q_{1T}}{Q_G} \frac{\chi_{32T}^2}{\chi_{32T}^2 + 1} \frac{Q_{2T}}{Q_L}. \quad (50)$$

It is noted that, also in this case, the optimization can be performed without communication with the receiving side. In fact, for constant values of k_{32} and R_L , G_P is also constant and, according to (34), in order to maximize G_T it is necessary to maximize P_{in} .

The feasibility of the solution expressed in (49) imposes:

$$Q_{1T} > \frac{\chi_{32T}^2 + 1}{Q_3}. \quad (51)$$

This means that by acting on the transmitting side, it is possible to maximize G_T for values of Q_{1T} satisfying (51), this being equivalent to impose an upper limit to R_G . In more detail, the upper limit on R_G depends on k_{32} and lowers for increasing values of k_{13} ; hence, for a given value of R_L , the possibility of maximizing G_T by acting on k_{13} depends on k_{32} .

It is worth noticing that the expression (50) of $G_{T,13}^M$ can be interpreted as the product of the efficiency of resonator 1 and the maximum transducer gain of the two-coil link formed by resonators 3 and 2 w.r.t. its load resistance (see the Appendix for the expression of G_T for a two-coil link).

Accordingly, the coupled resonators 1 and 3 transform the R_G into the reflected impedance

$$R_{R,in} = \frac{(\omega_0 M_{13})^2}{R_G + R_1} = \frac{X_0 n_{32}^2}{Q_3} (\chi_{32T}^2 + 1), \quad (52)$$

which is equal to the input resistance of the link formed by resonators 3 and 2. This means that k_{13}^{GT} realizes the power-matching condition at the input port of the link formed by

coils 3 and 2. As in the previous case, it can be noted that in these conditions, the input port impedance of the three-coil link is not matched. In fact, for $k_{13} = k_{13}^{GT}$ it results

$$R_{in} = X_0 n_{12}^2 \left(\frac{2}{Q_1} + \frac{1}{Q_G} \right) = R_G + 2R_1, \quad (53)$$

hence R_{in} becomes equal to the generator resistance only if the TX resonator losses tend to zero.

3) DISCUSSION ON THE RESULTS

The analyses performed in the previous section show that:

- By keeping fixed the coupling factor between the transmitter and the relay element k_{13} , it is possible to vary k_{32} to optimize the efficiency (i.e. G_P) and the power on the load (i.e. G_T) provided that the conditions expressed in (38) and in (42) are satisfied, while it is not possible to optimize the available gain G_A .
- By keeping fixed the coupling factor between the relay element and the receiver k_{32} , it is possible to vary k_{13} to optimize the power on the load and the available gain G_A provided that the conditions expressed in (51) and in (47) are satisfied, while it is not possible to optimize the efficiency.

It should be pointed out that, since in neither case it is possible to optimize both the available and the transducer gain, only local maxima of the transducer gain, and consequently of the output power, can be achieved. In order to overcome these limitations, it is appropriate to investigate the behavior of a WPT link with two relay elements.

Additionally, according to the expressions (37), (41), (46), (50) of the maximized gains, it can be concluded that case B is equivalent to consider the problem of the cascade of two links: one with a variable coupling (i.e. the one formed by resonator 3 and either resonator 1 or 2) and one with a fixed coupling (i.e. the one formed by resonator 3 and either resonator 2 or 1). The link with a variable coupling is used as a matching network, where the variable coupling is exploited in order to maximize one of the gains of the link with fixed coupling. Accordingly:

- When the goal is to maximize G_T , the optimum value of the variable coupling is the one which realizes the power-matching condition at either the input or the output ports of the fixed link.
- When the goal is to maximize G_A or G_P , the optimum value of the variable coupling is the one which realizes, for the fixed link, its conjugate image impedance at either the input (maximization of G_A) or output port (maximization of G_P).

V. NUMERICAL VERIFICATION

In order to verify the theory reported in the previous sections, circuital simulations have been performed with the

Table 3. Data of the coils.

f_0 (MHz)	R_G (Ω)	R_L (Ω)	L_1 (μ H)	L_2 (μ H)	L_3 (μ H)	C_1 (pF)	C_2 (pF)	C_3 (pF)	Q_1	Q_2	Q_3	k_{13}	k_{32}
13.56	10	5	0.9	0.4	0.4	153.07	344.40	344.40	255	177	177	0.2	0.22

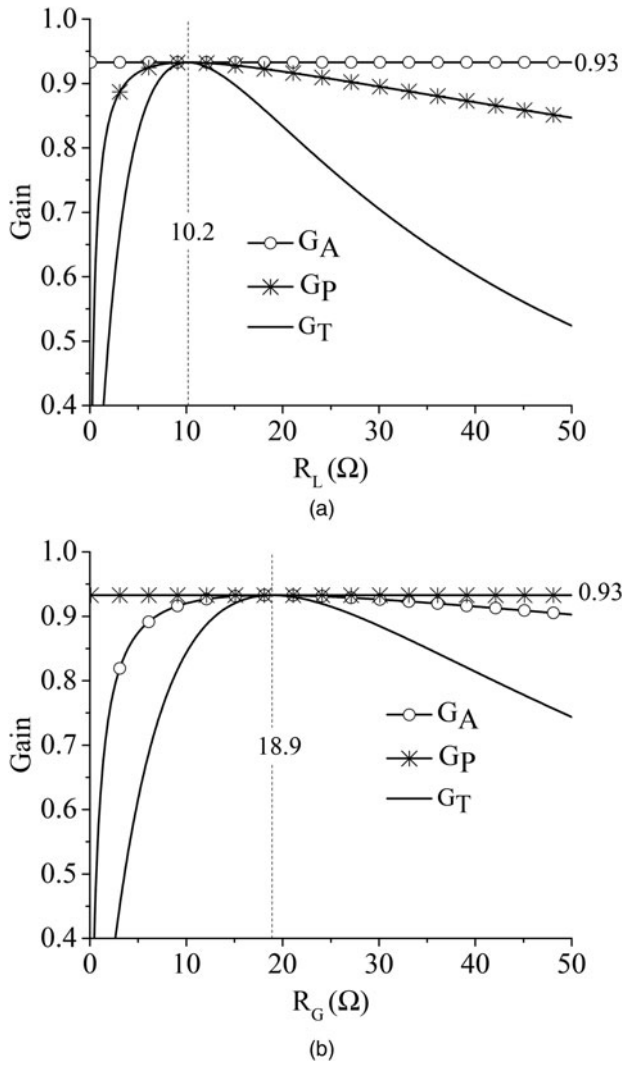


Fig. 4. Results obtained from circuital simulations for G_T , G_P , and G_A by varying: (a) the value of R_L for $R_G = R_{i1}$, (b) the value of R_G for $R_L = R_{i2}$. The values assumed for k_{13} and k_{32} are 0.2 and 0.22, respectively.

commercial tool NI AWR design environment. The value assumed for the coils are reported in Table 3 and were taken from [27] (see Table 2).

First of all, simulations were performed in order to verify that it is possible to maximize all the three gains by setting $R_G = R_{i1}$ and $R_L = R_{i2}$. To this end, simulations were performed:

- by setting $R_G = R_{i1} = 18.9 \Omega$ and by varying R_L (see Fig. 4a),
- by setting $R_L = R_{i2} = 10.2 \Omega$ and by varying R_G (see Fig. 4b).

It can be seen that circuital simulations confirm the theory; in fact, the three gains are maximized for $R_G = R_{i1}$ and $R_L = R_{i2}$. It can be also seen that for $R_G = R_{i1}$ and $R_L = R_{i2}$, the gains assume the same value: $G_T = G_A = G_P = G_M = 0.93$. Additionally, as expected, G_A is independent of R_L while G_P is independent of R_G . As per G_P , the dependence on both R_G and R_L is highlighted in Fig. 5.

Later on, simulations were performed by varying the values of k_{13} and k_{32} . The results obtained this way for G_P , G_T , and G_A are given in Figs 6–8. According to the theoretical analysis,

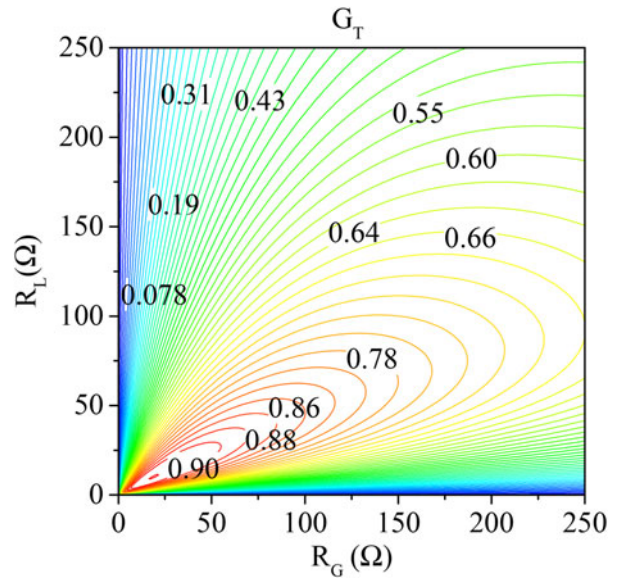


Fig. 5. Results obtained from circuital simulations for G_T by varying R_G and R_L . The values assumed for k_{13} and k_{32} are 0.2 and 0.22, respectively.

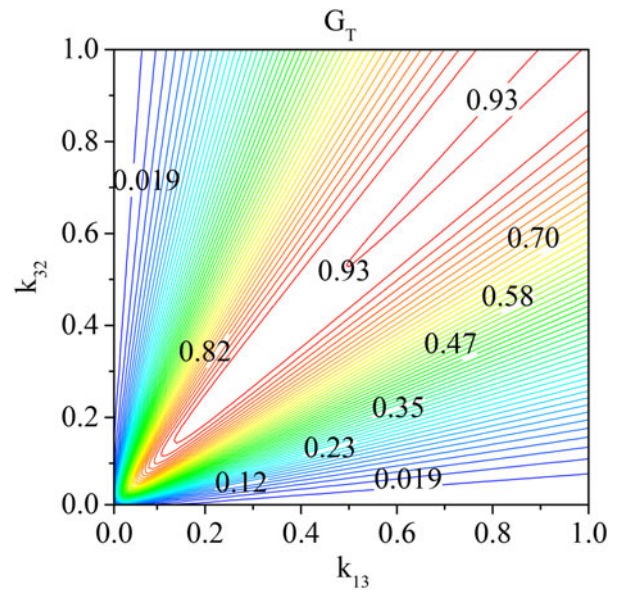


Fig. 6. Results obtained from circuital simulations for the available gain G_T by varying the values of k_{13} and k_{32} . The values assumed for R_G and R_L are 10Ω and 5Ω , respectively.

it can be seen that for a given value of k_{13} , G_P and G_T can be maximized by an appropriate selection of the value of k_{32} , while it can be seen that G_A keeps growing as k_{32} increases.

In the same figures, it is also evident that by acting on k_{13} for a given value of k_{32} it is possible to maximize G_T and G_A , while G_P continues to increase as k_{13} increases. The same behavior can be observed in Figs 9–11, where the results calculated for $R_G = 5 \Omega$ and $R_L = 200 \Omega$ are reported. The intrinsic limits of the three-coil configuration are particularly evident in Fig. 10, where it can be seen that for k_{32} lower than 0.2 very low values of G_P are obtained for any value of k_{13} . By comparing Figs 7 and 10, it can be also seen that, according to (38), for a given value of k_{13} , the value of k_{32} which allows

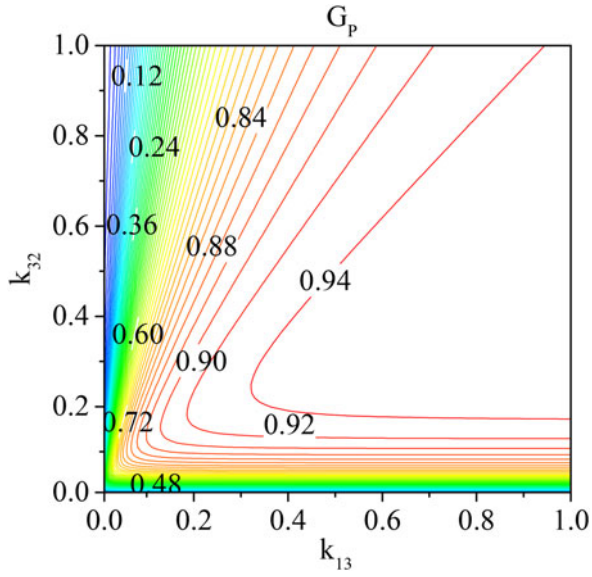


Fig. 7. Results obtained from circuital simulations for the available gain G_p by varying the values of k_{13} and k_{32} . The values assumed for R_G and R_L are 10Ω and 5Ω , respectively.

maximizing G_p increases with R_L . In particular, according to (38), for the case analyzed in Fig. 10 (i.e. $R_G = 5\Omega$ and $R_L = 200\Omega$), the value of k_{32} which allows maximizing G_p is not physically realizable for $k_{13} > 0.14$.

It is worth observing that the ratio between the transducer gain and the power gain is an indicator of the level of matching at the input port of the network with respect to the generator with internal resistance R_G ; in fact, G_T/G_p is the portion of the power available from the generator that is transferred to the network:

$$\frac{G_T}{G_p} = \frac{P_{in}}{P_{AG}}. \quad (54)$$

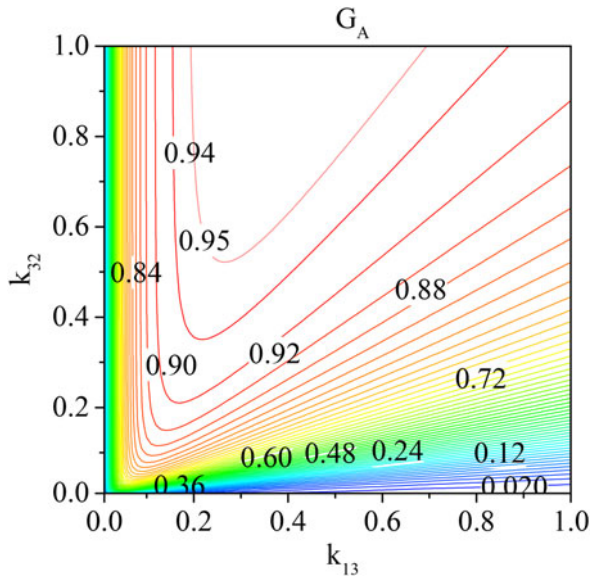


Fig. 8. Results obtained from circuital simulations for the available gain G_A by varying the values of k_{13} and k_{32} . The values assumed for R_G and R_L are 10Ω and 5Ω , respectively.

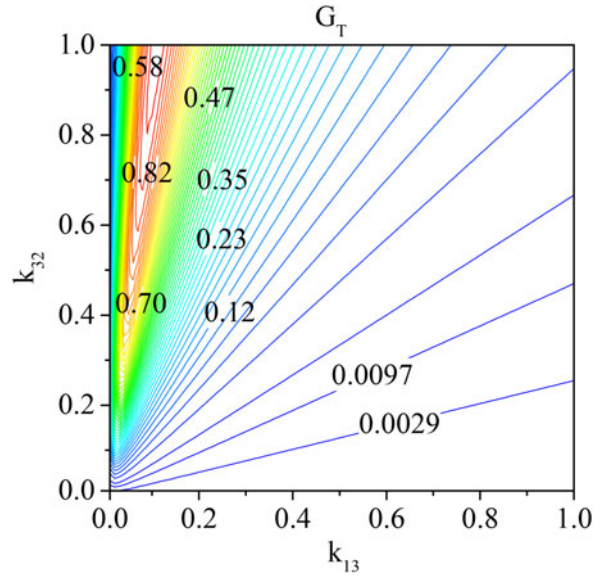


Fig. 9. Results obtained from circuital simulations for the available gain G_T by varying the values of k_{13} and k_{32} . $R_G = 5\Omega$ and $R_L = 200\Omega$.

Similarly, the ratio between the transducer gain and the available gain is an indicator of the level of matching at the output port of the network with respect to the load R_L ; in fact, G_T/G_A is the portion of the maximum available load power which is delivered to the given load R_L :

$$\frac{G_T}{G_A} = \frac{P_L}{P_A}. \quad (55)$$

The results obtained by circuital simulations are given in Figs 12–15; in more detail, Figs 12 and 13 refer to $R_G = 10\Omega$ and $R_L = 5\Omega$, while Figs 14 and 15 refer to $R_G = 5\Omega$ and $R_L = 200\Omega$.

From these figures, it can be seen that the dependence of G_T/G_p and G_T/G_A on the couplings k_{13} and k_{23} is the same

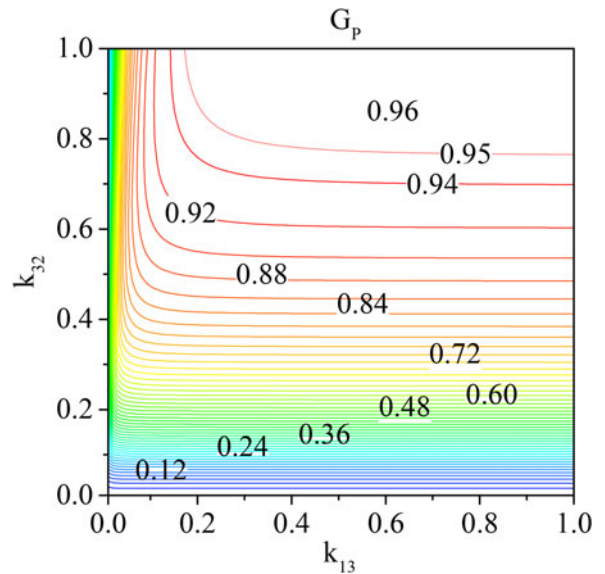


Fig. 10. Results obtained from circuital simulations for the available gain G_p by varying the values of k_{13} and k_{32} . $R_G = 5\Omega$ and $R_L = 200\Omega$.

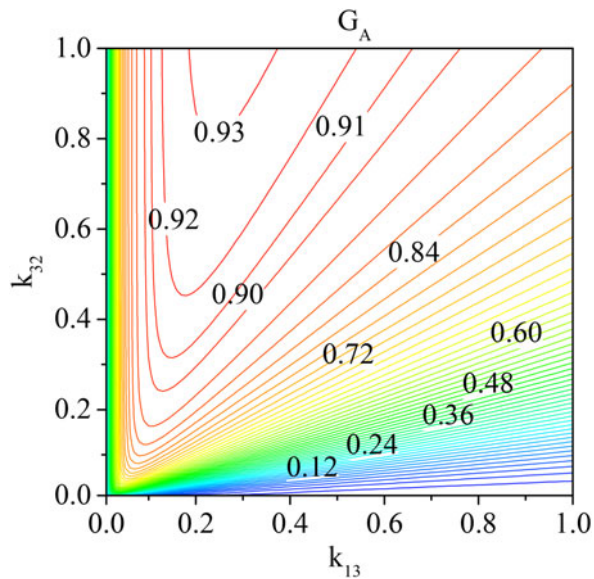


Fig. 11. Results obtained from circuital simulations for the available gain G_A by varying the values of k_{13} and k_{32} . Results obtained for $R_G = 5\Omega$ and $R_L = 200\Omega$.

calculated for G_T ; in fact, in order to maximize the power delivered to the load, it is necessary to maximize both G_T/G_P and G_T/G_A .

Finally, for the sake of comparison with [27], in Fig. 16, the results achieved in using k_{32} to keep the power gain to its maximum value while the load is varying are reported. The figure shows the data provided by the analytical formulas for k_{32}^{GP} as function of the load resistance R_L ; the corresponding G_P is also reported. It can be easily verified that the results reported in Fig. 16 are in agreement with those reported in Fig. 5b of [27]. According to (38), by adjusting the value of k_{32} it is possible to maintain G_P to its maximum value for values of R_L satisfying the following relation:

$$R_L < R_2 \left(\frac{Q_2 Q_3}{\sqrt{\chi_{13}^2 + 1}} - 1 \right), \quad (56)$$

which, for the analyzed case, leads to an upper limit for R_L of about 935Ω . In Fig. 16, the results obtained from circuital simulations and validating the theory are also reported.

Similar considerations are valid with regard to the use of k_{13} to keep the available gain to its maximum value while the generator impedance R_G is varying. The data calculated from analytical formulas for k_{13}^{GA} as function of R_G are given in Fig. 17 and compared with circuital simulation results.

According to (47), by varying the value of k_{13} it is possible to maintain G_A to its maximum value for values of R_G below

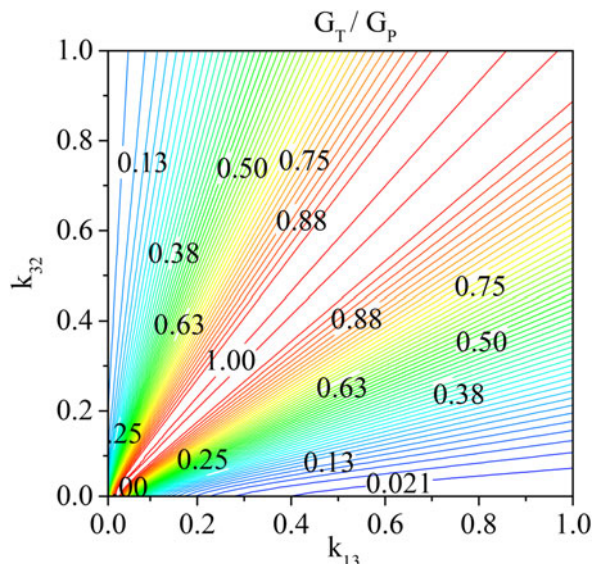


Fig. 12. Results obtained from circuital simulations for the ratio between the transducer gain G_T and the power gain G_P by varying the values of k_{13} and k_{32} . Results obtained for $R_G = 10\Omega$ and $R_L = 5\Omega$.

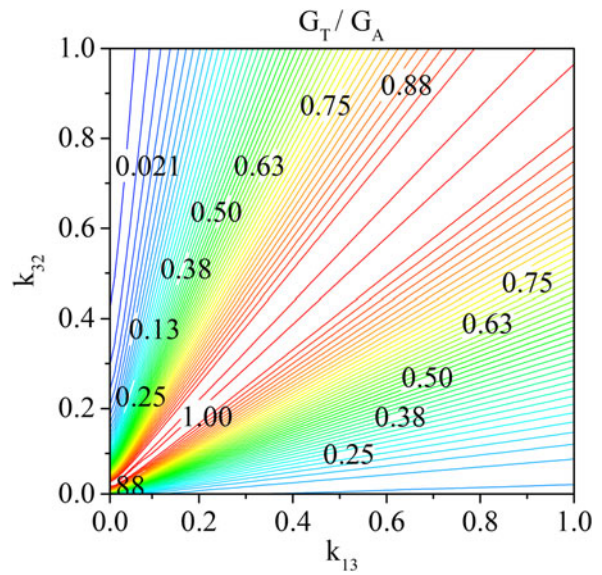


Fig. 13. Results obtained from circuital simulations for the ratio between the transducer gain G_T and the available gain G_A by varying the values of k_{13} and k_{32} . Results obtained for $R_G = 10\Omega$ and $R_L = 5\Omega$.

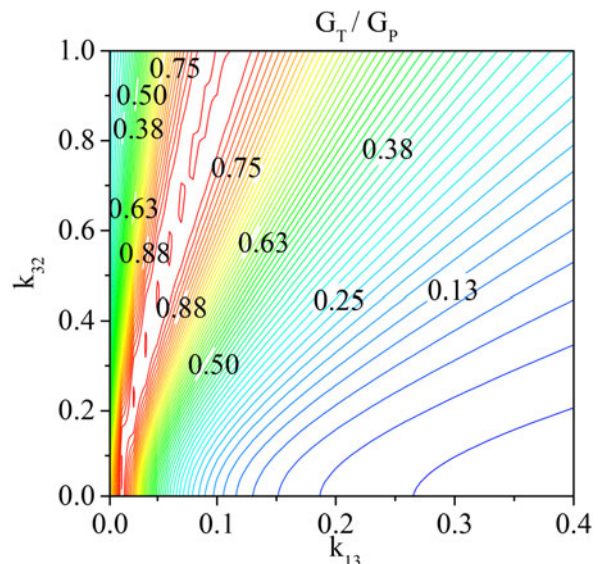


Fig. 14. Results obtained from circuital simulations for the ratio between the transducer gain G_T and the power gain G_P by varying the values of k_{13} and k_{32} . Results obtained for $R_G = 5\Omega$ and $R_L = 200\Omega$.

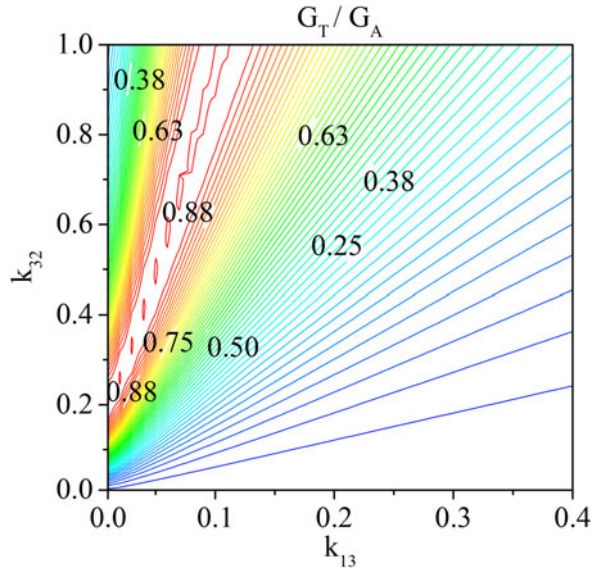


Fig. 15. Results obtained from circuital simulations for the ratio between the transducer gain G_T and the available gain G_A by varying the values of k_{13} and k_{32} . Results obtained for $R_G = 5\Omega$ and $R_L = 200\Omega$.

the upper limit expressed by:

$$R_G < R_1 \left(\frac{Q_1 Q_3}{\sqrt{\lambda_{32}^2 + 1}} - 1 \right), \quad (57)$$

which, for the present case, is equal to about 3821Ω .

VI. CONCLUSION

The problem of magnetic resonant WPT between one transmitter and one receiver coupled through a relay element has been considered from a rigorous network viewpoint. Given the network parameters, the problem of maximizing the performance of the network has been analytically solved. In more detail, the link performance has been described by using the

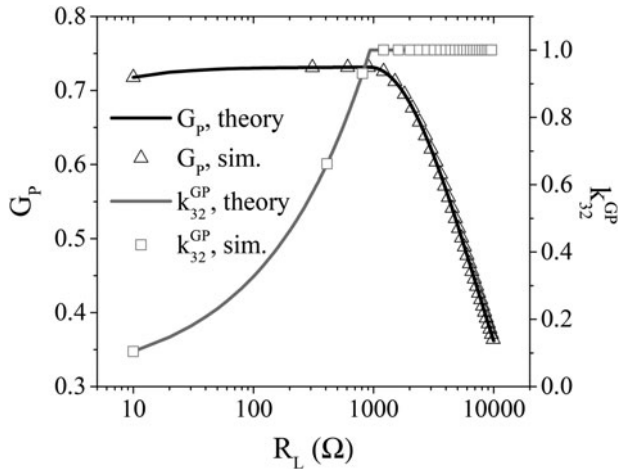


Fig. 16. Results obtained for k_{32}^{GP} and the corresponding G_p as function of R_L . The value assumed for k_{13} is 0.03 . The figure shows a comparison between data provided by the analytical formulas and the results obtained by circuital simulations.

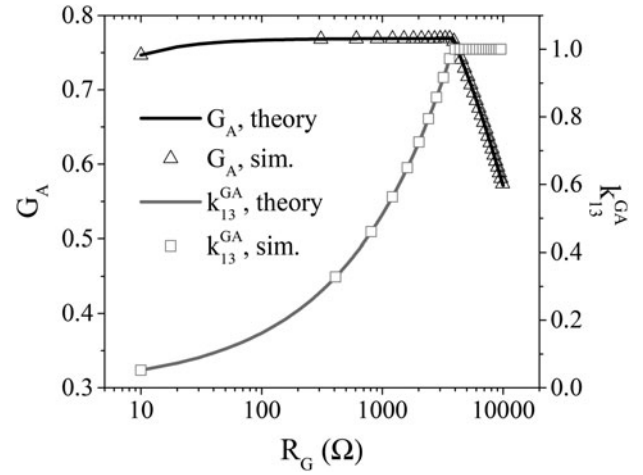


Fig. 17. Results obtained for k_{13}^{GA} and the corresponding G_A as function of R_G . The value assumed for k_{32} is 0.1 . The figure shows a comparison between data provided by the analytical formulas and the results obtained by circuital simulations.

standard gain definitions available for a two-port network: power, available, and transducer gain. It has been shown that the definition usually adopted in the WPT context for the efficiency is equivalent to the power gain of the network and that, for given values of the available power of the generator, maximizing the power on the load is equivalent to maximize the transducer gain.

For the analyzed case, it has been shown that the impedance matrix is purely resistive and, as a consequence, the conjugate image impedances are simply the image resistances. Accordingly, in the case of given parameters of the link it has been shown that it is possible to maximize all the gains by setting the generator and the load impedance equal to the image resistances of the network. As per the case where the load and the source are given, one of the couplings (e.g. the coupling between the transmitter and the relay element or the coupling between the relay element and the receiver) can be set in order to satisfy the requirement on the distance to be covered by the link and the other one can be optimized to maximize one of the three network gains. However, the results reported in this paper demonstrate that the possibility of analytically maximizing the available gain and the power gain depends on which of the two couplings of the relay element, the one with the transmitter or the one with the receiver, is considered as a degree of freedom.

In particular, from analytical formulas and circuital simulations, it has been shown that when the coupling between the transmitter and the relay element is fixed, it is not possible to

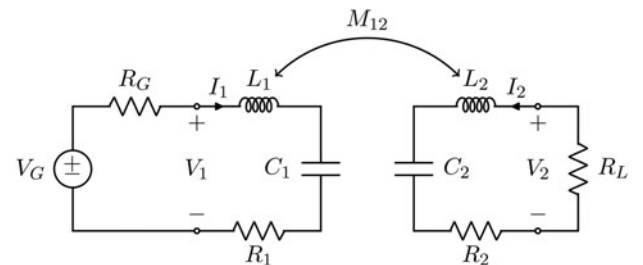


Fig. 18. Schematic representation of a two-coil WPT link.

Table 4. Definitions.

$X_o = \omega_o L_2$	$n_{12} = \sqrt{\frac{L_1}{L_2}}$	$k_{12} = \frac{M_{12}}{\sqrt{L_1 L_2}}$
$Q_i = \frac{\omega_o}{R_i}$	$Q_G = \frac{\omega_o L_1}{R_G}$	$Q_L = \frac{\omega_o L_2}{R_L}$
$Q_{1T} = \frac{Q_1 Q_G}{Q_1 + Q_G}$	$Q_{2T} = \frac{Q_2 Q_L}{Q_2 + Q_L}$	$\chi_{12} = \sqrt{Q_1 Q_2} k_{12}$
$\chi_{1T2} = \sqrt{Q_{1T} Q_2} k_{12}$	$\chi_{12T} = \sqrt{Q_1 Q_{2T}} k_{12}$	$\chi_{1T2T} = \sqrt{Q_{1T} Q_{2T}} k_{12}$

maximize the available gain G_A , which keeps growing for increasing values of the coupling between the relay element and the receiver. Similarly, for a given value of the coupling between the relay element and the receiver, it has been shown that it is not possible to find the absolute maximum of the efficiency (i.e. the power gain G_P). In fact, G_P increases for increasing values of the coupling between the relay element and the transmitter.

Since, in order to achieve the maximum transducer gain, and consequently the maximum output power, it is necessary to maximize both the available and the power gain, only a local maximum can be obtained for G_T by using just one relay element.

REFERENCES

- [1] Costanzo, A.; et al. Electromagnetic energy harvesting and wireless power transmission: a unified approach. *Proc. IEEE*, **102** (11) (2014), 1692–1711.
- [2] Bird, T.S.; Rypkema, N.; Smart, K.W.: Antenna impedance matching for maximum power transfer in wireless sensor networks, in *IEEE Sensors*, Amsterdam, Netherlands, 25–28 Oct. 2009, 916–919.
- [3] Imura, T.; Okabe, H.; Hori, Y.: Basic experimental study on helical antennas of wireless power transfer for electric vehicles by using magnetic resonant couplings, in *Proc. of Vehicle Power and Propulsion Conference*, Dearborn, MI, USA, 7–10 Sept. 2009, 936–940.
- [4] Monti, G.; Arcuti, P.; Tarricone, L.: Resonant inductive link for remote powering of pacemakers. *IEEE Trans. Microw. Theory Tech.*, **63** (11) (2015), 3814–3822.
- [5] Monti, G.; Dionigi, M.; Mongiardo, M.; Perfetti, R.: Optimal design of wireless energy transfer to multiple receivers: power maximization. *IEEE Trans. Microw. Theory Tech.*, **65** (1) (2017), 260–269.
- [6] Del Prete, M.; Costanzo, A.; Georgiadis, A.; Collado, A.; Masotti, D.; Popovic, Z.: Energy-autonomous Bi-directional Wireless Power Transmission (WPT) and energy harvesting circuit, in *IEEE MTT-S Int. Microwave Symp. (IMS)*, Phoenix, AZ, USA, 2015, 1–4.
- [7] Li, S.; Mi, C.C.: Wireless power transfer for electric vehicle applications. *IEEE J. Emerging Sel. Top. Power Electron.*, **3** (1) (2015), 4–17.
- [8] Karalis, A.; Joannopoulos, J.D.; Soljačić, M.: Efficient wireless non-radiative mid-range energy transfer. *Ann. Phys.*, **323** (1) (2008), 34–48.
- [9] Monti, G.; et al. Wireless power transfer between one transmitter and two receivers: optimal analytical solution. *Wireless Power Transf.*, **3** (2016), 63–73.
- [10] Dionigi, M.; Mongiardo, M.; Perfetti, R.: Rigorous network and full-wave electromagnetic modeling of wireless power transfer links. *IEEE Trans. Microw. Theory Tech.*, **63** (1) (2015), 65–75.
- [11] Aditya, K.; Williamson, S.S.: A review of optimal conditions for achieving maximum power output and maximum efficiency for a series-series resonant inductive link. *IEEE Trans. Transp. Electrification*, **3** (2) (2017), 303–311.
- [12] Mirbozorgi, S.A.; Yeon, P.; Ghovanloo, M.: Robust wireless power transmission to mm-sized free-floating distributed implants. *IEEE Trans. Biomed. Circuits Syst.*, **11** (3) (2017), 692–702.
- [13] Monti, G.; Costanzo, A.; Matri, F.; Mongiardo, M.; Tarricone, L.: Rigorous design of matched wireless power transfer links based on inductive coupling. *Radio Sci.*, **51** (6) (2016), 858–867.
- [14] Zhang, F.; Hackworth, S.A.; Fu, W.; Li, C.; Mao, Z.; Sun, M.: Relay effect of wireless power transfer using strongly coupled magnetic resonances. *IEEE Trans. Magn.*, **47** (5) (2011), 1478–1481.
- [15] Hui, S.Y.R.; Zhong, W.; Lee, C.K.: A critical review of recent progress in mid-range wireless power transfer. *IEEE Trans. Power Electron.*, **29** (9) (2014), 4500–4511.
- [16] Monti, G.; Tarricone, L.; Dionigi, M.; Mongiardo, M.: Magnetically coupled resonant wireless power transmission: An artificial transmission line approach, in *Proc. of the Microwave Conf. (EuMC)*, Amsterdam, Netherlands, Oct. 2012, 233–236.
- [17] Monti, G.; Corchia, L.; Tarricone, L.; Mongiardo, M.: A network approach for wireless resonant energy links using relay resonators. *IEEE Trans. Microw. Theory Tech.*, **64** (10) (2016), 3271–3279.
- [18] Luo, B.; Wu, S.; Zhou, N.: Flexible design method for multi-repeater wireless power transfer system based on coupled resonator bandpass filter model. *IEEE Trans. Circuits Syst. I Regul. Pap.*, **61** (11) (2014), 933–942.
- [19] Ahn, D.; Hong, S.: A study on magnetic field repeater in wireless power transfer. *IEEE Trans. Ind. Electron.*, **60** (1) (2013), 360–371.
- [20] Sun, T.; Xie, X.; Li, G.; Gu, Y.; Deng, Y.; Wang, Z.: System with an efficiency-enhanced power receiver for motion-free capsule endoscopy inspection. *IEEE Trans. Biomed Eng.*, **59** (11) (2012), 3247–3253.
- [21] Zhong, W.; Lee, C.K.; Hui, S.Y.R.: General analysis on the use of Tesla’s resonators in domino forms for wireless power transfer. *IEEE Trans. Ind. Electron.*, **60** (1) (2013), 261–270.
- [22] Kurs, A.; Karalis, A.; Moffatt, R.; Joannopoulos, J.D.; Fisher, P.; Soljacic, M.: Wireless power transfer via strongly coupled magnetic resonances. *Science*, **317** (5834) (2007), 83.
- [23] Lee, G.; Waters, B.H.; Shi, C.; Park, W.S.; Smith, J.R.: Design considerations for asymmetric magnetically coupled resonators used in wireless power transfer applications, in *IEEE Topical Conf. on Biomedical Wireless Technologies, Networks, and Sensing Systems (BioWireless)*, Austin, TX, USA, 2013, 1–3.
- [24] Kim, J.; Son, H.-C.; Kim, K.-H.; Park, Y.-J.: Efficiency analysis of magnetic resonance wireless power transfer with intermediate resonant coil. *IEEE Antennas Wireless Propag. Lett.*, **10** (2011), 389–392.
- [25] Lee, B.; Kiani, M.; Ghovanloo, M.: A triple-loop inductive power transmission system for biomedical applications. *IEEE Trans. Biomed. Circuits Syst.*, **10** (1) (2016), 138–148.
- [26] Zhong, W.; Zhang, C.; Liu, X.; Hui, S.: A methodology for making a three-coil wireless power transfer system more energy efficient than a two-coil counterpart for extended transfer distance. *IEEE Trans. Power Electron.*, **30** (2) (2015), 3288–3297.
- [27] Kiani, M.; Jow, U.-M.; Ghovanloo, M.: Design and optimization of a 3-coil inductive link for efficient wireless power transmission. *IEEE Trans. Biomed. Circuits Syst.*, **5** (6) (2011), 579–591.
- [28] Shimada, A.; Ito, Y.; Uehara, H.; Ohira, T.: Effect of hop counts on power division ratio in multi-hop power transfer via magnetic resonance, in *IEEE Wireless Power Transfer Conf.*, Perugia, Italy, 2013, 179–184.

- [29] Monti, G.; Costanzo, A.; Mastri, F.; Mongiardo, M.: Optimal design of a wireless power transfer link using parallel and series resonators. *Wireless Power Transf.*, 3 (2) (2016), 105–116.
- [30] Roberts, S.: Conjugate-Image Impedances. *Proc. of the IRE*, 34 (4) (1946), 198–204.

APPENDIX: EXPRESSIONS OF THE GAINS FOR A TWO-COIL WPT LINK

In this section, the expressions of the three gains for a two-coil WPT link are briefly recalled. It is assumed that the link, which is depicted in Fig. 18, is fed by a sinusoidal voltage generator V_G with internal resistance R_G and is connected to a load resistance R_L . The symbols defined in Table 4, which have similar meanings to those defined for the three-coil case, are used in the analysis.

The equations for the two coils are given by

$$\begin{aligned} V_1 &= R_1 I_1 + j\omega_0 M_{12} I_2, \\ V_2 &= j\omega_0 M_{12} I_1 + R_2 I_2. \end{aligned} \quad (\text{A.1})$$

Hence, making use of the definitions reported in Table 4, the elements of the impedance matrix of the two-coil link can be expressed as

$$z_{11} = r_{11} = \frac{X_0 n_{12}^2}{Q_1}, \quad (\text{A.2})$$

$$z_{12} = z_{21} = jx_{12} = j \frac{X_0 n_{12}}{\sqrt{Q_1 Q_2}} \chi_{12}, \quad (\text{A.3})$$

$$z_{22} = r_{22} = \frac{X_0}{Q_2}. \quad (\text{A.4})$$

If the terminating impedances are assumed to be purely resistive, the input and output impedances provided by (3) and (5) are also resistive, and can be expressed as

$$R_{in} = \frac{X_0 n_{12}^2}{Q_1} (\chi_{12T}^2 + 1), \quad (\text{A.5})$$

$$R_{out} = \frac{X_0}{Q_2} (\chi_{1T2}^2 + 1). \quad (\text{A.6})$$

Since z_{11} and z_{22} are real, while z_{12} and z_{21} are imaginary, the conjugate image impedances of the two-coil link reduce to the image resistances, and can be computed by (18) and (19) as

$$R_{i1} = \frac{X_0 n_{12}^2}{Q_1} \sqrt{\chi_{12}^2 + 1}, \quad (\text{A.7})$$

$$R_{i2} = \frac{X_0}{Q_2} \sqrt{\chi_{12}^2 + 1}. \quad (\text{A.8})$$

Making use of the general formulas reported in Table 2, it is possible to derive the expressions of the power gain

$$G_P = \frac{\chi_{12T}^2}{\chi_{12T}^2 + 1} \frac{Q_{2T}}{Q_L}, \quad (\text{A.9})$$

of the available gain

$$G_A = \frac{Q_{1T}}{Q_G} \frac{\chi_{1T2}^2}{Q_{1T2}^2 + 1}, \quad (\text{A.10})$$

and of the transducer gain

$$G_T = \frac{Q_{1T}}{Q_G} \frac{4\chi_{1T2T}^2}{(\chi_{1T2T}^2 + 1)^2} \frac{Q_{2T}}{Q_L}. \quad (\text{A.11})$$

The three gains are maximized when $R_G = R_{i1}$ and $R_L = R_{i2}$. In these conditions, the common value of the gains is

$$G_M = \frac{(1 - \sqrt{\chi_{12}^2 + 1})^2}{\chi_{12}^2}. \quad (\text{A.12})$$

In addition, the following considerations can be made:

- for a fixed given R_L , the maximum of G_T w.r.t. R_G is obtained when R_G is equal to the input resistance (A.5), and in these conditions, the trasducer gain becomes equal to the power gain (A.9);
- for a fixed given R_G , the maximum of G_T w.r.t. R_L is obtained when R_L is equal to the output resistance (A.6), and in these conditions, the trasducer gain becomes equal to the available gain (A.10).



Franco Mastri received the Laurea degree (100/100 cum laude) in Electronic Engineering from the University of Bologna, Italy, in 1985. From 1990 to 2004, he was a Research Associate with the Department of Electrical Engineering, University of Bologna, where he has been an Associate Professor of electrotechnics

since 2005. His main research interests include non-linear circuit simulation and design techniques (with special emphasis on CAD techniques for large-size problems), non-linear RF device modeling, non-linear/RF co-simulation of RF systems, stability and noise analysis of non-linear circuits.



Mauro Mongiardo (F'11) has received the Laurea degree (110/110 cum laude) in Electronic Engineering from the University of Rome "La Sapienza" in 1983. In 1991, he became an Associate Professor of Electromagnetic Fields, and from 2001, he is a full Professor of Electromagnetic Fields at the University of Perugia. He has been elected Fellow of

the IEEE "for contributions to the modal analysis of complex electromagnetic structures" in 2011. The scientific interests of

Mauro Mongiardo have concerned primarily the numerical modeling of electromagnetic wave propagation both in closed and open structures. His research interests have involved CAD and optimization of microwave components and antennas.

Mauro Mongiardo has served in the Technical Program Committee of the IEEE International Microwave Symposium from 1992. From 1994, he is a member of the Editorial Board of the IEEE TRANSACTIONS ON MICROWAVE THEORY AND TECHNIQUES. During the years 2008–2010, he has been an Associate Editor of the IEEE TRANSACTIONS ON MICROWAVE THEORY AND TECHNIQUES. He is an author or co-author of over 200 papers and articles in the fields of microwave components, microwave CAD, and antennas. He is the co-author of the books “Open Electromagnetic Waveguides” (IEE, 1997) and “Electromagnetic Field Computation by Network Methods” (Springer, 2009).



Giuseppina Monti (SM'16) Giuseppina Monti received the Laurea degree in Telecommunication Engineering (with honors) from the University of Bologna, Italy, in 2003, and the Ph.D. in Information Engineering from the University of Salento (Italy), in 2007. She is currently with the Department of Innovation Engineering

(University of Salento), where she is a temporary Researcher and Lecturer in CAD of Microwave circuits and Antennas. Her current research interest includes the analysis and applications of artificial media (such as, for instance, double-negative metamaterials and nano-carbontube), the analysis of electromagnetic compatibility and electromagnetic interference problems in planar microwave circuits, the design and realization of: microwave components and MEMS-based reconfigurable antennas and devices, rectenna systems, systems and devices for wireless power transmission applications. She has co-authored a chapter of a book and about 100 papers appeared in international conferences and journals.



Marco Dionigi (M'14) has received the Laurea degree (110/110 cum laude) in Electronic Engineering from the University of Perugia. He achieved at the same university the title of Ph.D. In 1997, he became an Assistant Professor at the Faculty of Engineering of the University of Perugia. He took part in several research projects regarding the develop-

ment of software tools for waveguide and antenna fullwave simulation, the development of permittivity and moisture microwave sensors, the development of an SAR and ultrawideband antennas. He was a coauthor of a paper awarded of the “Young Engineers Prize” at the European Microwave Conference 2005 in Paris. He is now involved in the study and development of high-efficient wireless electromagnetic power transfer for industrial applications. He is an author of more than 70 papers on international journal and conferences.



Luciano Tarricone (SM'11) received the Laurea degree in Electronic Engineering (cum laude) and Ph.D. degree from the Rome University “La Sapienza,” Rome, Italy, in 1989 and 1994, respectively. From 1990 to 1992, he was a Researcher with the IBM Rome Scientific Centers. From 1992 to 1994, he was with the IBM European Center for Scientific

and Engineering Computing, Rome, Italy. Between 1994 and 1998, he was a Researcher with the University of Perugia, Perugia, Italy, and, between 1998 and 2001, he was a “Professore Incaricato” of electromagnetic (EM) fields and EM compatibility. Since November 2001, he has been a Faculty Member with the Department of Innovation Engineering, University of Salento, Lecce, Italy, where he is a full Professor of EM fields and coordinates a research group of about 15 people. He has authored and coauthored approximately 300 scientific papers. His main contributions are in the modeling of microscopic interactions of EM fields and biosystems, and in numerical methods for efficient CAD of microwave circuits and antennas. He is currently involved in bioelectromagnetics, electromagnetic energy harvesting and wireless power transmission, novel CAD tools and procedures for microwave circuits, RFID, and EM high-performance computing.